Efficient Pose Deformations for Human Models in Customized Sizes and Shapes

Shuaiyin Zhu and P.Y. Mok*
Institute of Textiles and Clothing, The Hong Kong Polytechnic University
Hunghom, Hong Kong.
sy.zhu@connet.polyu.hk; *tracy.mok@polyu.edu.hk

ABSTRACT

Modelling dynamic pose deformations of human subjects is an important topic in many research applications. Existing approaches of human pose deformations can be classified as volume-based, skeletal animation and example-based methods. These approaches have both strengths and limitations. However, for models in customized shapes, it is very challenging to deform these models into different poses rapidly and realistically. We propose a conceptual model to realize rapid and realistic pose deformation to customized human models by the integration of skeletal-driven rigid deformation and example-learnt non-rigid surface deformation. Based on this framework, a method for rapid automatic pose deformation is developed to deform human models of various body shapes into a series of dynamic poses. A series of algorithms are proposed to complete the pose deformation automatically and efficiently, including automatic segmentation of body parts and skeleton embedding, skeletal-driven rigid deformation, training of non-rigid deformation from pose dataset; shape mapping of non-rigid deformation, and integration of rigid and non-rigid deformations. Experiment has shown that the proposed method can customize accurate human models based on two orthogonal-view photos and also efficiently generate realistic pose deformations for the customized models.

Keywords

Human modelling, pose deformation, example-based approach, model customization, deformation transfer

1. INTRODUCTION

3D human body modelling is needed in many research applications, such as gaming, filming, medical, ergonomics and fashion. Modelling human body has two major aims: shape and pose modelling. A number of methods have been developed to address these two aims. For example, methods or applications [2-5,19] were reported to estimate global shape and pose model of human subjects using image or depth information as input deform a parametric model. Example-learnt parametric model can capture global shape and pose deformation realistically, and thus have used in many computer graphic applications. However, for fashion or ergonomic related research applications, the key focus of human modelling is accurate body shape of the resulting models. Parametric deformable models may not be able to accurately capture the shape details of individuals. This is because example-based methods often learn parametric deformable models form examples using Principal Component Analysis (PCA), resulting in models of 'average' looks, missing local shape characteristics of individuals. The existing human modelling methods could not address to the specific needs of fashion industry, where not only global features but also local details of the individual's body figures are precisely modelled.

We present an automatic method of customizing human body shape model from images, and deforming the customized model in different poses. We mainly follow the method of [13] for customizing accurate body shape of individuals from images, which is a complete automatic method from image processing to model deformation. However, [13] addressed to shape modelling of individuals from images only, however the customised model holds a standard standing post. In addition to shape customization, we propose a new method to deform the customized shape model into different dynamic poses. The rest of the paper is organized as follows. First, the related work of human shape and pose modelling will be reviewed in Section 2. The detailed of the proposed method will be described in Section 3, including shape customization and pose deformation. Section 4 shows some model customization results together with thorough discussion on the pros and cons of the current method. Section 5 concludes this paper and also suggestion the future work.

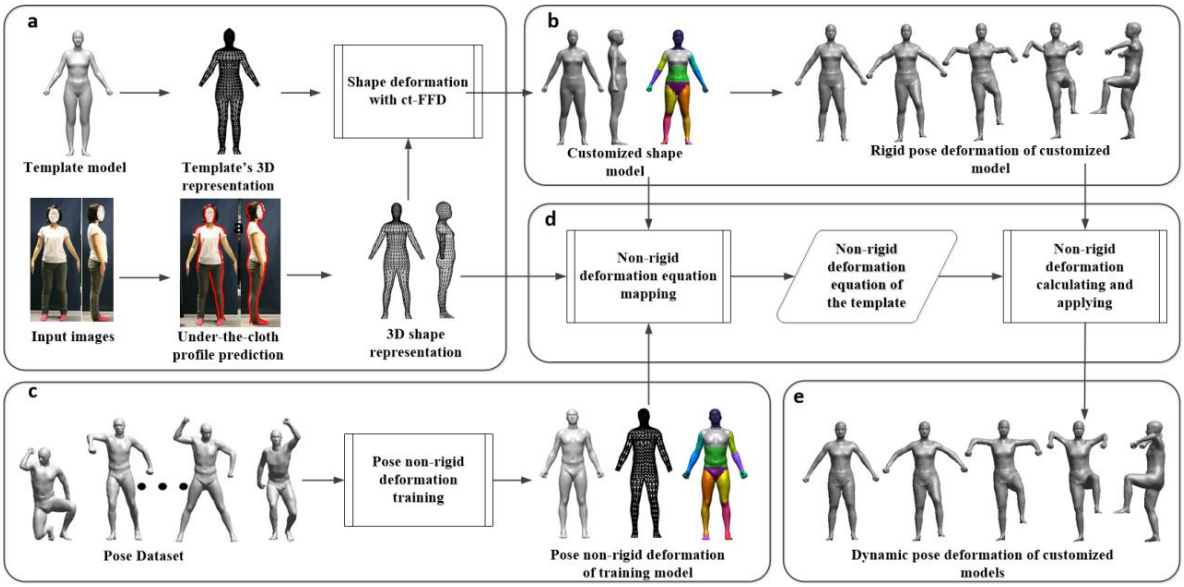

Figure 1. Dynamic pose modelling of customized human models – Method Overview

2. RELATED WORK

Existing approaches of modelling realistic pose deformations of human subjects can be classified as volume-based, skeletal animation and example-based methods. Volume-based methods [14,17] were proposed in the early stage of pose modeling research. Volume-based methods were based on physical analysis of muscle or tissue, anatomy and biomechanics theory. In volume-based pose deformation, the skeleton of a virtual 3D human body model, which includes bones, muscle, tissue and skin, was first deformed using motion data. The skeleton was used to compute the forces on the correlated muscle or tissue. The muscle and tissue deform according to computed forces, and so does the skin. Volume-based methods not only achieve realistic skin deformation but also compute the forces and kinematics of the correlated muscle or tissue. Volume-based methods are widely used in biomechanics research. However, these methods are all computationally expensive, and the pose deformation is not real-time. Furthermore, a detailed model of a human subject with skeleton, muscle and tissues is complex to create. The calculation of pose deformation for a standard model (in standard size and shape) is already tedious and time-consuming, and it is very difficult, if not impossible, to calculate the pose deformation of human models in customized shapes.

Direct-deformation methods were later proposed to model pose deformation as skin deformation, without modeling the bones, muscles and tissues under the skin. Direct-deformation methods can be classified into two categories: skeletal animation and example-driven methods. Magnenat-Thalmann [11] introduced the first skeletal animation algorithm that deforms a human hand with the assistance of virtual finger bones. The Linear Blending Skinning (LBS) algorithm [9], one of the most well-known skeletal animation algorithms, was introduced around the same time. Compared to volume-based methods, LBS provides a rapid solution for pose deformation. Thus, LBS is widely applied in game development and computer animation. However, the resulting skins of LBS algorithms have an unnatural appearance because of missing muscle deformation. Some skeletal animation algorithms were proposed to improve LBS [6-7,12,18]. For example, [18] described an enhanced skeletal animation algorithm called multi-weight enveloping (MWE), which replaces the linear model with a statistical model for the skin surface and the corresponding joints' deformation. MWE can generate realistic skin deformation if the deformed pose is within the training dataset. Other well-known extensions of LBS includes Spherical Blend Skinning [7] and Dual Quaternion blending Skinning [8]. In sum, skeletal animation algorithms provide solutions for rapid pose deformation, but the shape accuracy of the deformed model is questionable, especially in the case of large joint angle changes.

Example-driven pose deformations [2,10,12,15,18] were introduced in the last decade or so, by taking advantage of scanning technology development and the availability of scanning data. For example, [1] described the first example-driven method that trains scanned human models in different poses. More recently, SCAPE [2] was introduced to deform the shape and pose of a template model. However, example-based methods that model shape deformation in a global space are not good at

customizing local shapes. Besides, example-based methods generate erroneous deformation in the case of a subject with a shape out of the scope of the training dataset. It is thus not ideal to deform customized models into different poses.

Recently, some researchers proposed to use motion data for shape modelling or mapping [22,23], while we propose to use images in this paper. Pons-Moll [25] developed a novel approach to model the soft-tissue deformations of full-body human models using 4D capture system. It used example-based approach for volume-based deformation, adding more detailed precise pose modelling for different subjects.

3. METHOD

3.1 Method Overview

Figure 1 shows an overview of human modelling method, it integrate shape modelling and pose modelling of human subjects. It involves a shape modelling method of individuals based on two orthogonal-view photos (as shown in (a) of the figure); and a pose modelling method, which integrates rigid deformation and non-rigid deformation (shown as (b-e) of the figure).

3.2 Shape Customization

We describe here an automatic method that constructs a 3D shape model of an individual based on his/her front-view and side view photos. The detailed method has been reported in [13]. Our method of shape customization defined a feature-aligned 3D shape representation to characterize human body physique in detail (refer to (a) of Figure 1). The 3D shape representation is a layered structure, each layer represents a cross-sectional shape of the subject's body at a specific level.

A layered structure with parallel cross-sections is an effective shape representation for clothing applications, because such a structure aligns with the clothing size definition. The parallel cross-sections characterize *local features* of the body in terms of *shape and size*, as some cross-sections indeed correspond to important body girth measurements, such as the bust, waist, and hip. The shape of these cross-sections gives detailed information on where the body has developed fat, for instance the shape of the waist girth.

Different from the example-based methods, which acquired global shape variations from full body scans, our shape customization method is capable of capturing and modelling the local body shape characteristics of individuals, by learning the cross-sectional size and shape relationships from over 10000+ scanned models using neural networks. Our method extract 2D body features from subjects' orthogonal-view photograph, from which to predict the cross-sectional shape in 3D, and then to reconstruct the overall 3D shape representation. Without assuming linear shape deformation, the method is able to capture local shape characteristics and has been applied to customize 3D body models for subjects dressed in tight-fit clothing [20] or dressed in arbitrary clothing, even loose-fit clothing [21]. The recent advancement of the shape modelling method is that new algorithms were developed to extract all features needed for the shape customization process from input images. These 2D features can identify and align with the 3D layered structure of shape representation accurately using anthropometric knowledge [13]. It implies that the accurate 3D models can be customized from input images in a complete automatic manner. The experimental results showed that output human models (both males and females) have accurate sizes (anthropometric measurements) and realistic shape details. The size measurement discrepancies between the resulting models and the scanned models are less than 2cm in all key girth measurements like bust, waist and hip.

3.3 Pose Deformation

As shown in Figure 1, we propose to model dynamic pose deformation to any customized model as an integration of pose-induced rigid deformation and non-rigid deformation. Rigid deformation here represents the deformation induced by different body parts' rotation and translation, such as forearms or lower legs. The deformation of these body parts explains most of the global change in body shapes in different dynamic pose deformations. In rigid deformation, a human model is deformed like a puppet, and such deformations are modeled as the rotation of different body parts along an articulated skeleton. Realistic skin surface deformation due to different pose change is obvious very different from rotation of an articulated model, and we model such skin surface differences as non-rigid deformations. We use the pose dataset of [2], which has a wide range of scan of a single subject in different poses. All scan models are properly registered, meaning that they have the same topology structure. The pose dataset in fact provides examples of realistic skin surface deformations, we can obtain non-rigid deformation to each triangle by computing the differences between rigidly deformed mesh and the corresponding pose model in the pose dataset. We then learn a regression model to predict non-rigid deformations using motion data. Our idea of pose modeling is similar to that of SCAPE [2], but we improve the detailed implementation in different areas, which will be explained in details below.

Pose deformation is modelled with reference to each triangle of a mesh model (template). Such formulation enables easy representation of deformation by matrix operations:

$$\tilde{\mathbf{V}}_k = \mathbf{T}\mathbf{V}_k^0 = \mathbf{T}_{L(k)}^R \mathbf{T}_k^Q \mathbf{V}_k^0 . \quad (1)$$

As shown in Equation (1), each triangle $\mathbf{V}_k^0$ of the template is multiplied by transformation matrix $\mathbf{T}$ to obtain its pose deformation, where $\mathbf{T}$ is a matrix product of two components $\mathbf{T}_{L(k)}^R$ and $\mathbf{T}_k^Q$. $\mathbf{T}_k^Q$ represents non-rigid pose-induced deformations specific to triangle $\mathbf{V}_k^0$ of the template; $\mathbf{T}_{L(k)}^R$ denoted the rotation of the rigid body part in the articulated skeleton, where $L(k)$ denotes the rigid part that triangle $\mathbf{V}_k^0$ is belonged to. Both $\mathbf{T}_k^Q$ and $\mathbf{T}_{L(k)}^R$ are functions of motion data, represented as joint rotation angles of a defined skeleton structure.

3.3.1 Rigid pose deformation

To obtain rigid deformation of a human model, the first step is to group triangle faces of the human mesh model into different rigid parts. Automatically grouping triangle surfaces is a typical mesh surface clustering problem. There are many different algorithms reported in the literature to recover articulated object models from meshes. In the vast majority of the applications, the articulated skeleton structure and its parameters have to be manually specified. In the SCAPE method, object surface segmentation is done by iteratively finding decomposition of the object surface into rigid parts and finding the location of the parts based on a set of registered 3D scans in different configurations [2]. They estimated the locations of the joints from the resulting segmentation. Their algorithm not only recovered the parts and the joints, but also figured out the optimal number of parts numerically. However, the availability of a sample of object instances is a necessary input in the SCAPE method for mesh segmentation. Moreover, recovering articulated skeleton as a numerical optimization problem from the sample scans may not result in parts that aligned well with human body features, and its segmentation results may vary when different dataset is used. Numerically optimized part number may result in skeleton structure different from the typical skeleton definition for animation applications.

We develop an efficient and automatic method that segments triangle faces of the mesh model into meaningful rigid parts, using the 3D shape representation constructed in the phase of shape modeling. The 3D shape representation has included a number of body features defined based on anatomical knowledge. We thus assign the triangle faces of 3D shape representation with a rigid part label $a_j \in \{a_1,\ldots,a_N\}$. We assign part labels based on the skeleton definition of the SCAPE model with a total of 16 rigid parts $\{a_1,\ldots,a_{16}\}$. However, it is important to note our method is flexible in term of the definition of skeleton structure, because we define using anatomical knowledge with identified body features of the 3D shape representation, which can be viewed as a simplified version of human model. In other words, we can model pose deformation using other skeleton structure definition that allow easy integration with motion data.

Given a customized human model in Figure 2(a), we can construct a 3D shape representation for the mesh model with faces labelled, as shown in Figure 2(b). Based on the labelled 3D shape representation, we calculate the correspondence relationship and assign part label for every triangle face of the customized human model with the following equations.

$$L(k) = L(a_j) \quad (2a)$$

such that

$$\arg \min_{\{a_1,\ldots,a_N\}} \left\| c_k - a_j \right\|^2 + \varphi(N(c_k), N(a_j)) \quad (2b)$$

In equation (2a), $L(k)$ denotes the centroid position c_k of triangle *k* on the human model, and a_j denotes the centroid position of the *j*-th triangle of the 3D shape representation. $L(a_j)$ records the part label $a_j \in \{a_1,\ldots,a_N\}$ that Equation (2b) is minimized. In Equation (2b), $\varphi(\cdot)$ is penalty function defined as

$$\varphi(N(c_k), N(a_j)) = \begin{cases} 0, & \text{if angle between } N(c_k) \text{ and } N(a_j) < 90^\circ; \\ \infty, & \text{else.} \end{cases} \quad (2c)$$

where function $N(c_k)$ calculates the normal vector of the triangle *k* at its centroid c_k. The penalty function $\varphi(\cdot)$ filters those triangles with different normal vectors, especially at connecting areas of two or more rigid parts, e.g. armpit. We only segment the 3D shape representation once, because the topology structure of 3D shape representation is the same for all customized human models. Figure 2(c) shows the result of segmenting input human model (a) into rigid parts.

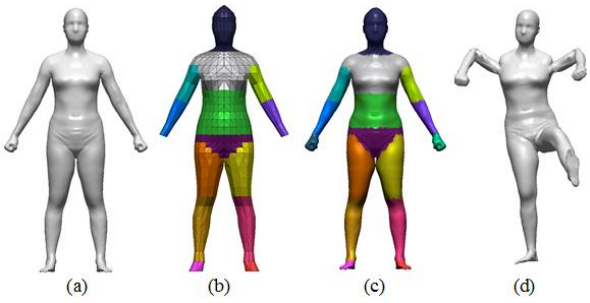

Figure 1. Part grouping and rigid part deformation.

3.3.2 Training of Non-rigid pose deformation

Since pose-induced non-rigid deformation for a customized model is unknown, we use the concept of deformation transferring [16] to copy the deformation from known pose dataset to the customized model. In addition to the given poses in the pose dataset, we train a model, using the pose dataset, to predict the non-rigid deformation of triangle *k*, namely the transformation matrix $\mathbf{T}_k^Q$ in Equation (1), using two adjacent joints' rotations, $\Delta r_{L(k),1}$ and $\Delta r_{L(k),2}$. Again, the formulation of non-rigid deformation is toward each triangle, $\tilde{\mathbf{V}}_k = \mathbf{T}_k^Q \mathbf{V}_k^0$.

The detailed formulation of non-rigid deformation is described as follows. We predict non-rigid deformation from articulated human pose, which is represented by a set of relative joint rotations. With a specific pose (*i*), the non-rigid deformation for every triangle *k* of the mesh is denoted by a 3×3 matrix

$$\mathbf{T}_k^{Q(i)} = \begin{bmatrix} q_{k,11}^i & q_{k,12}^i & q_{k,13}^i \\ q_{k,21}^i & q_{k,22}^i & q_{k,23}^i \\ q_{k,31}^i & q_{k,32}^i & q_{k,33}^i \end{bmatrix} \quad (3)$$

We reduce the dimensionality of the problem by assuming $\mathbf{T}_k^{Q(i)}$ is affected by two adjacent joints of the rigid part where triangle k is belonged to. Each entry $q_{k,mn}^i$ of matrix $\mathbf{T}_k^{Q(i)}$ is thus inner product of two vectors:

$$q_{k,mn}^i = [\Delta r_{L(k),1}^i \; \Delta r_{L(k),2}^i \; 1] \cdot \mathbf{b}_{k,mn}^i \quad m,n=1,2,3 \quad (4)$$

where $\mathbf{b}_{k,mn}^i$ is a 7×1 column vector of linear weights that map the rotations of two adjacent joint angles ($\Delta r_{L(k),1}^i$, $\Delta r_{L(k),2}^i$) and a constant bias term as the entry value of transformation matrix $\mathbf{T}_k^{Q(i)}$. Each joint rotation $\Delta r_{L(k),1}^i$ can be easily computed from the absolute rotation matrices of the two rigid parts, and be specified by three parameters in twist coordinates.

The goal is to learn the parameters $\mathbf{b}_{k,mn}^i$ in Equation (4). We train this non-rigid deformation prediction model using SCAPE pose dataset. We construct the 3D shape representation for the SCAPE template at standard pose (pose zero) of the pose dataset. We next segment this SCAPE template into rigid parts and extract skeleton structure accordingly. We then obtain the rigid deformations of the SCAPE template by rigid part rotation $\mathbf{T}^{R(i)}$ for all pose instances (*i*) given in the pose dataset, using the method described in Section 7.2.3 above.

Each mesh model in the pose dataset is the final shape integrating both rigid $\mathbf{T}^{R(i)}$ and non-rigid $\mathbf{T}^{Q(i)}$ pose deformations. Given transformation for each mesh instance $\mathbf{T}_k^{Q(i)}$ and its rigid part rotation $\mathbf{T}_{L(k)}^{R(i)}$, solving for the 9×7 regression parameters $\mathbf{b}_{k,mn}^i$ for each triangle *k* is straightforward by minimizing a quadratic cost function

$$\arg\min_{\mathbf{b}_{k,mn}^i} \sum_{i=1}^{m} ([\Delta r_{L(k),1}^i \; \Delta r_{L(k),2}^i \; 1] \cdot \mathbf{b}_{k,mn}^i - q_{k,mn}^i)^2 \quad (5)$$

To solve Equation (5), we performed PCA on the observed joint rotation angles ($\Delta r_{L(k),1}^i$, $\Delta r_{L(k),2}^i$), reducing the size of the problem because many human joints only have one or two degree of freedom instead of three. With learned parameters $\mathbf{b}_{k,mn}^i$, we can calculate using Equation (4) the non-rigid deformation matrix $\mathbf{T}_k^{Q(i)}$ based on pose/motion data, in terms of joint rotation angles. Figure 2 shows the examples of pose deformation of SCAPE template. These poses are not given in pose dataset, but new poses synthesized completely from a vector of joint rotations.

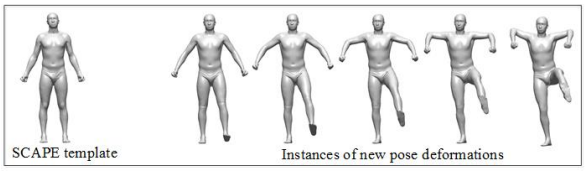

Figure 2. Pose deformation of the SCAPE template with synthesized joint rotations.

3.3.3 Pose deformation of customized human models

We model realistic skin surface deformation induced by different dynamic poses (defined in terms of joint rotation angles) using a pose dataset on a template mesh. The next question to answer is how realistic pose deformation can be obtained for a customized human model. We use the concept of deformation transfer that transfers the deformations of the SCAPE model (source) to the customized model (target).

the application of deformation transfer technique requires the availability of pairwise correspondence between source and target meshes. In general, with a set of users selected marker points, pairwise correspondence are determined by deforming target mesh into a shape of the source and then by calculating the closest Euclidean distance between the source mesh and the deformed target mesh. Such deformation is iteratively improved. Well known correspondence searching algorithms include Iterated Closet Points (ICP) [1][16] and Correlated Correspondence [2]. The selection of marker points requires some manual work at the initial stage and the involvement of manual work also causes the final results depend on users' selection or experience.

We propose a completely automatic correspondence alignment method for human models using the shape modeling method developed early. Our correspondence mapping involves three simple steps: 1) construct 3D shape representations for the source mesh (SCAPE template) and target mesh (customized human model); 2) deform the source mesh using ct-FFD [20] based on the 3D shape representation of the target; 3) for each triangle *k* of the target mesh, seek the triangle on the deformed source mesh so that centroids of the two triangles are in the closest proximity. This can be done by Equation (2b), except the different definitions of a_j, which denotes the centroid position of the *j*-th triangle face of the source mesh (SCAPE template) instead of the 3D shape representation. There are no restrictions on the correspondence mapping, and it can be injective, surjective, or bijective.

Our method in fact automatically identifies all the marker points without any manual operations. It ensures fine alignment with human body features, and the process is not iterative. By eliminating iterative deformations, our method is very efficient to register two human models. Table 1 compares the time spent by ICP method and our method for registering SCAPE template with a target mesh of 23112 triangles. It is shown that our method is much more efficient than ICP in correspondence mapping.

Table 1 Time comparison of registration methods

Registration methods	ICP (1 iteration)	ICP (6 iterations)	ct-FFD-based
Time spent (Mesh with12428 vertices and 23112 triangles)	24s (Core i7/8GB Memory/ Matlab)	229s (Core i7/8GB Memory/ Matlab)	5.1s (Core i7/8GB Memory/ Matlab)

Upon establishing correspondence between SCAPE template and a customized model, we can transfer pose-induced non-rigid deformation from the source mesh (SCAPE) to the target mesh (customized model) to finish dynamic pose deformations on customized model. This is done by setting the gradient of objective function

$$\arg\min_{\tilde{\mathbf{x}}} \left\| \mathbf{c} - \mathbf{A}\tilde{\mathbf{x}} \right\|_2^2 \qquad (5)$$

to zero, where $\tilde{\mathbf{x}}$ is a vector of unknown deformed vertex locations of customized model, **c** is a vector recording transformations of the mesh of the pose dataset, is is calculated as

$$\mathbf{c} = \mathbf{T}^R\mathbf{T}^Q = \mathbf{A}\tilde{\mathbf{x}} \qquad (6)$$

A of Equation (5) is a large, sparse matrix that the entries in **A** depends only on the target mesh's structure. In Equation (6), the rigid part transformation matrix $\mathbf{T}^R$ is known based on given motion data and once the part grouping result of the customized model is known. With the motion data, we also calculate the non-rigid deformation using the SCAPE model. For every customized model, the sparse matrix **A** in Equation (6) is known. We can then calculate dynamic pose deformation of the customized model accordingly by integrating non-rigid deformation and rigid part rotation by equation (1). Figure 3 shows the corresponding pose deformation transferred from SCAPE template in Figure 2. The resulting pose deformations on a customized model have natural and realistic skin surface deformation appearance similar to that of the source (Figure 2).

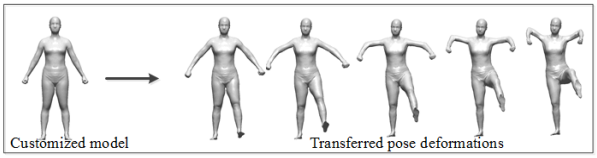

Figure 3. Resulting pose deformation on a customized model

4. RESULTS AND DISCUSSION

We evaluate the pose deformation by recruiting eight female and eight male subjects. These subjects can be classified into underweight, normal, overweight and obesity according to their BMI values. Figure 4 shows four examples of the shape customization results, which are compared to their scanned models. Figures 6 and 7 show, respectively, all female and male subjects' customized models in standard pose.

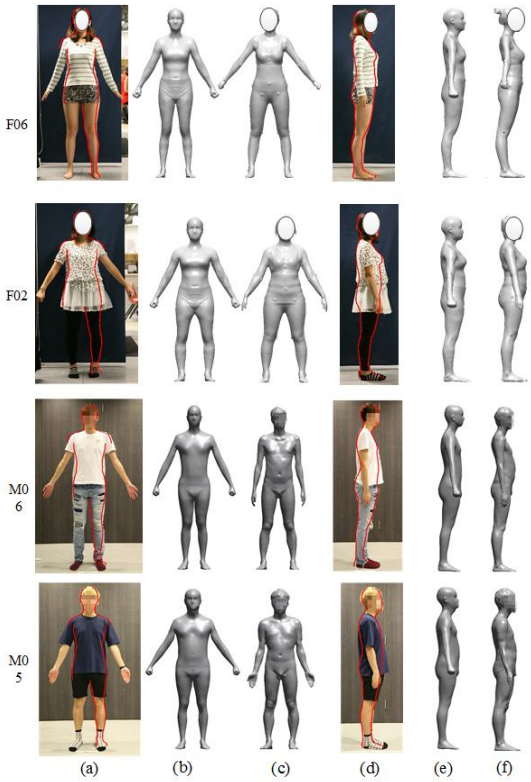

Figure 4. Four shape customization results

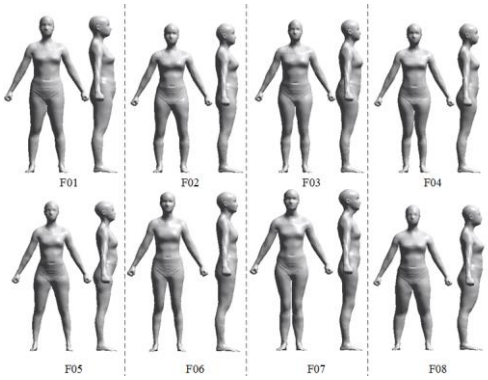

Figure 5. Female customized models in standard standing pose

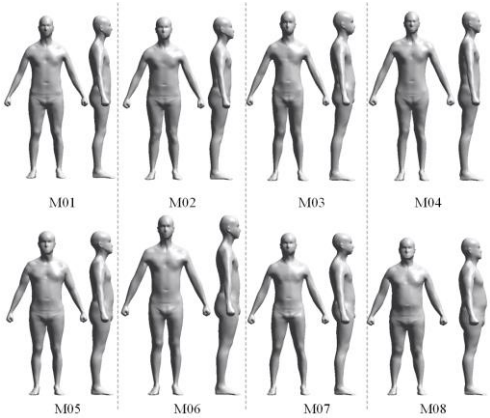

Figure 6. Male customized models in standard standing pose

We deformed all subjects' customized models into other poses dynamically. Figure 7 and Figure 8 show dynamic pose deformation examples of these subjects, and these poses are given in the pose dataset of SCAPE model. Comparing with the rigid part deformation based on the articulated models, our method generates realistic pose deformations on customized models, similar to that of the SCAPE model, even in poses with maximum bending angles.

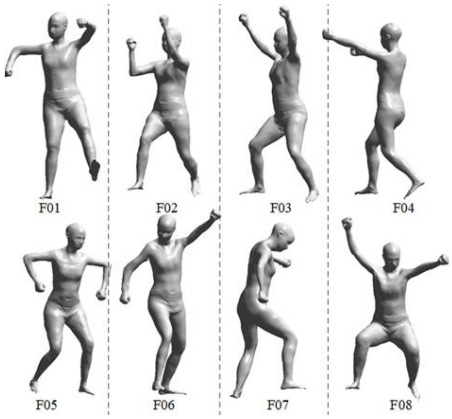

Figure 7. Dynamic deformed female models

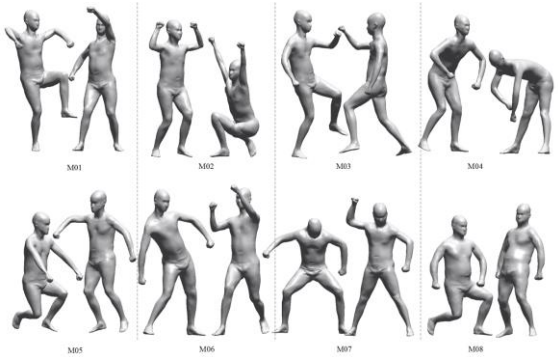

Figure 8. Dynamic deformed male models

In order to evaluate the pose deformation comprehensively, we scanned two female subjects in three different poses, as indicated on the right of Figure 9. We estimated their pose or skeleton data by manually select marker points from scanned models. Based on these pose data, we deformed the corresponding customized models as shown on the left of Figure 9.

As poses of scanned model are estimated, the estimated skeleton is not exactly equal to the real pose in the scans. Having said that, we can see the shape of the scanned models and the deformed models resembles, except some local areas, e.g. the chest areas. That is because the pose induced non-rigid deformation is transferred from the SCAPE model (a male scanned subject) to other customized models. Non-rigid deformation can be viewed as muscle deformation, yet the same muscle model is used for all people. Although the model can generate

realistic mesh models in a wide range of poses, the current method cannot capture the fact that more muscular people are likely to exhibit greater muscle deformation than others, and, conversely, that muscle deformation may be obscured in people with significant body fat.

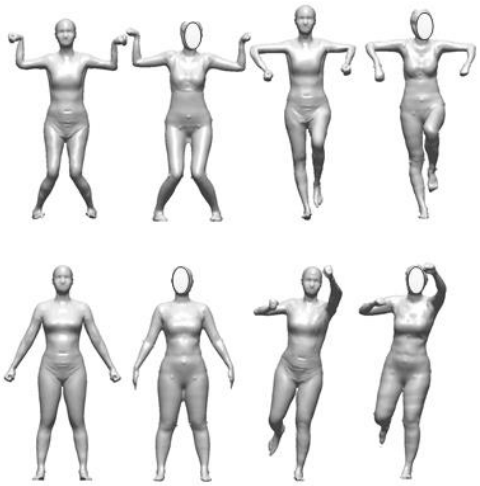

Figure 9. Comparison between pose deformation models and the corresponding scanned models

We can improve the current method using scans of different example subjects in different poses to learn the non-rigid deformation, and we transfer the deformation from one of the example subject that has the closest shape characteristic as that of the customized model.

5. CONCLUSION

We have presented human modelling method that automatically obtain 3D shape model using two orthogonal-view photographs. We also present an efficient method to deform any customized model into dynamic poses. Pose deformation is done by first grouping the triangles mesh of the customized model into articulated rigid parts with the assistance of 3D shape representation constructed in the step of shape modeling. Next, the human model is transformed in the form of rigid part rotations. Then, we learn the skin surface (non-rigid) deformations from a pose dataset to correct the defects in rigid deformation. The non-rigid deformation is transferred from pose dataset to the customized model so as to have realistic pose induced shape deformations on customized model. We optimize the procedures to realize very efficient pose deformations on customized models with diverse shapes.

6. ACKNOWLEDGMENTS

The work described in this paper was partially supported by a grant from the Research Grants Council of the Hong Kong Special Administrative Region, China (Project No. PolyU 5218/13E). The partial support of this work by the Innovation and Technology Commission of Hong Kong, under grant ITS/253/15, and The Hong Kong Polytechnic University, under project code: RPUC, are gratefully acknowledged.

7. REFERENCES

[1] Allen, B., Curless, B. & Popović, Z. (2002) Articulated body deformation from range scan data, ACM Transactions on Graphics, 21:1–8.

[2] Anguelov, D., Srinivasan, P., Koller, D., Thrun, S., Rodgers, J. & Davis, J. (2005) SCAPE, ACM Transactions on Graphics, 24(3), p. 408.

[3] Balan A., Sigal L., Black L., Davis J., and Haussecker. H. (2007). Detailed human shape and pose from images. IEEE Conference on Computer Vision and Pattern Recognition 2007 (CVPR '07), pp.1-8, 17-22 June 2007.

[4] Bogo, F., Black, M. J., Loper, M. and Romero, J. (2015). Detailed full-body reconstructions of moving people from monocular RGB-D sequences, Proceedings of the IEEE International Conference on Computer Vision, pp. 2300–2308.

[5] Guan, P.G.P., Weiss, A., Balan, A.O. and Black, M.J. (2009) Estimating human shape and pose from a single image, Computer Vision, IEEE 12th International Conference on Computer Vision.

[6] Kavan, L., & Zara, J. (2003). Real Time Skin Deformation with Bones Blending. In WSCG.

[7] Kavan, L. and Žára, J. (2005). Spherical blend skinning: a real-time deformation of articulated models, Proceedings of the 2005 symposium on Interactive 3D graphics and games, 1(212), pp. 9–16.

[8] Kavan, L., Collins, S., Žára, J. and O'Sullivan, C. (2008). Geometric skinning with approximate dual quaternion blending, ACM Transactions on Graphics, 27(4), pp. 1–23.

[9] Lander, J. (1999), Over my dead, polygonal body, Game Developer Magazine, (October), pp. 17–22.

[10] Lewis, J.P., Cordner, M. and Fong, N. (2000), Pose space deformation, Proceedings of the 27th annual conference on Computer graphics and interactive techniques - SIGGRAPH '00, pp. 165–172.

[11] Magnenat-Thalmann, N. R. Laperriere, and D. Thalmann, Joint-dependent local deformations for hand animation and object grasping, Proc. Graphics Interface'88, pp. 26–33, 1988.

[12] Mohr, A. and Gleicher, M. (2003) 'Building efficient, accurate character skins from

examples', ACM Transactions on Graphics, 22(3), p. 562.

[13] Mok P.Y. and Zhu SY. (2017), Precise shape estimation of dressed subjects from two-view image sets, In Calvin Wong (Ed.) Applications of Computer Vision in Fashion and Textiles, Elsevier.

[14] Nakamura, Y., Yamane, K., Suzuki, I. and Fujita, Y. (2003). Dynamic Computation of Musculo-Skeletal Human Model Based on Efficient Algorithm for Closed Kinematic Chains, Proceedings of the 2nd International Symposium on Adaptive Motion of Animals and Machines, p. SaP-I-2.

[15] Sloan, P.P.J., Rose, C.F. and Cohen, M.F. (2001). Shape by example, i3D - Interactive 3D Graphics and Games, pp. 135–143.

[16] Sumner, R. W. and Popović, J. (2004), Deformation transfer for triangle meshes, ACM Transactions on Graphics, 23(3), p. 399.

[17] Suzuki & Takatsu. (1997). 3D and 4D Visualization of Morphological and Functional Information from the Human Body Using Noninvasive Measurement Data, Atlas of Visualization, Vol 3..

[18] Wang, X. C. and Phillips, C. (2002) Multi-weight enveloping, Proceedings of the 2002 ACM SIGGRAPH/Eurographics symposium on Computer animation - SCA '02, p. 129.

[19] Weiss, A., Hirshberg, D. and Black, M.J. (2011), Home 3D body scans from noisy image and range data, Proceedings of the IEEE International Conference on Computer Vision, pp. 1951–1958.

[20] Zhu, S., Mok, P. Y. and Kwok, Y. L. (2013) An efficient human model customization method based on orthogonal-view monocular photos, CAD Computer Aided Design, 45(11), pp. 1314–1332.

[21] Zhu, S. and Mok, P. Y. (2015) 'Predicting Realistic and Precise Human Body Models Under Clothing Based on Orthogonal-view Photos', Procedia Manufacturing. Elsevier B.V., 3(Ahfe), pp. 3812–3819.

[22] Güdükbay, U., Demir, İ., & Dedeoğlu, Y. (2013). Motion capture and human pose reconstruction from a single-view video sequence. Digital Signal Processing, 23(5), 1441-1450.

[23] Gültepe, U., & Güdükbay, U. (2014). Real-time virtual fitting with body measurement and motion smoothing. Computers & Graphics, 43, 31-43.

[24] Pons-Moll, G., Romero, J., Mahmood, N., & Black, M. J. (2015). Dyna: A model of dynamic human shape in motion. ACM Transactions on Graphics (TOG), 34(4), 120.